On a method to predict extreme wave events

Peter Janssen

European Centre for Medium-Range Weather Forecasts

<peter.janssen@ecmwf.int>

Extreme wave event hitting the lower deck of Brent B. Crest height is 23 m.

Introduction

In this talk I will introduce the relatively new field of predicting extreme events caused by surface gravity waves on the ocean surface. They are called Rogue waves or Freak Waves. I will briefly indicate the main reasons why such extreme waves occur and then I will describe a **statistical** method to predict these extreme events.

Freak waves are basically caused by

- **Constructive interference** of **free** waves, giving steeper waves
- augmented by (nonlinear) processes such as
  - Benjamin-Feir Instability (**focussing** because waves temporary borrow energy from their neighbours). This process is only pronounced for narrow-band wave trains. May then give large deviations from Normality.
  - Wave-current interactions may increase steepness and therefore enhance the Benjamin-Feir instability.
  - **Bound** waves contribute to Skewness and Kurtosis as well

At sea, only a statistical description of the phenomena is possible because freak waves basically are similar to the luck of the draw in the lottery.

From knowledge of the wave spectrum one can determine all relevant statistical parameters such as skewness and kurtosis and from this one may evaluate the pdf of envelope wave height and maximum wave height. Here, **shallow water effects** will be emphasized.

Next, we discuss a fundamental mechanism that generates freak waves, namely the **Benjamin-Feir** Instability which is an example of a four-wave interaction: The linear dispersion relation for water waves is

$$\omega(k) = \sqrt{gk \tanh kD}$$

with ω angular frequency, $k = |\mathbf{k}|$ wavenumber and D the water depth. This dispersion relation allows a resonant four-wave interaction which is determined by the conditions
$\omega_1 + \omega_2 = \omega_3 + \omega_4$ and $\mathbf{k}_1 + \mathbf{k}_2 = \mathbf{k}_3 + \mathbf{k}_4$.

By means of a graphical construction it can be shown that resonant three wave interactions do not exist for surface gravity waves.

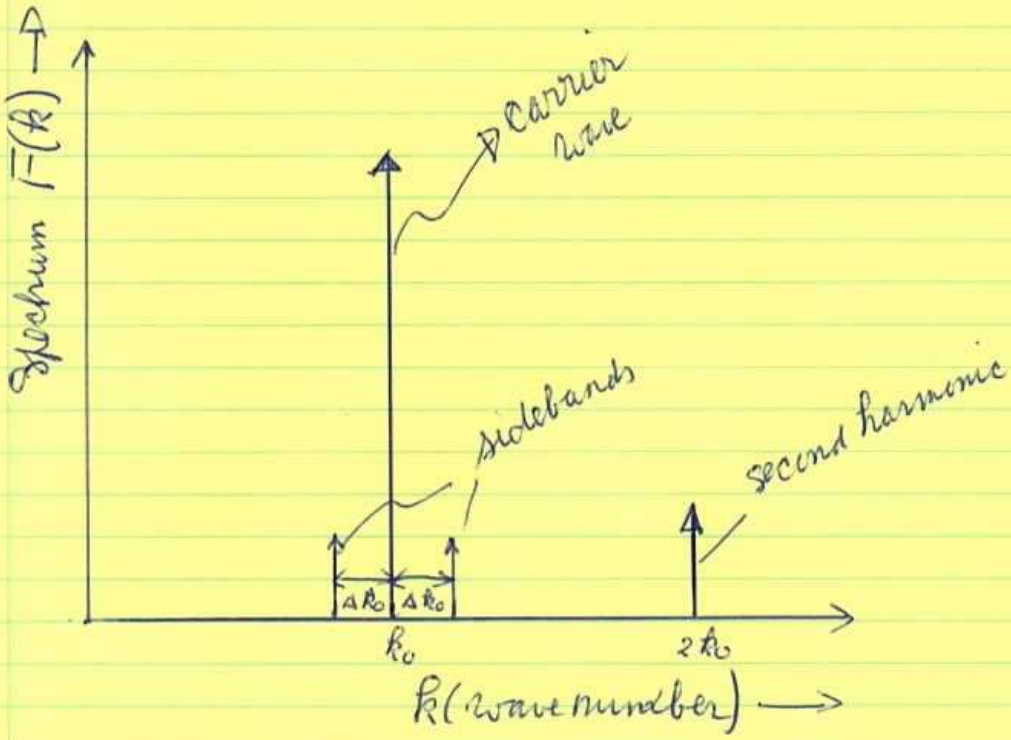

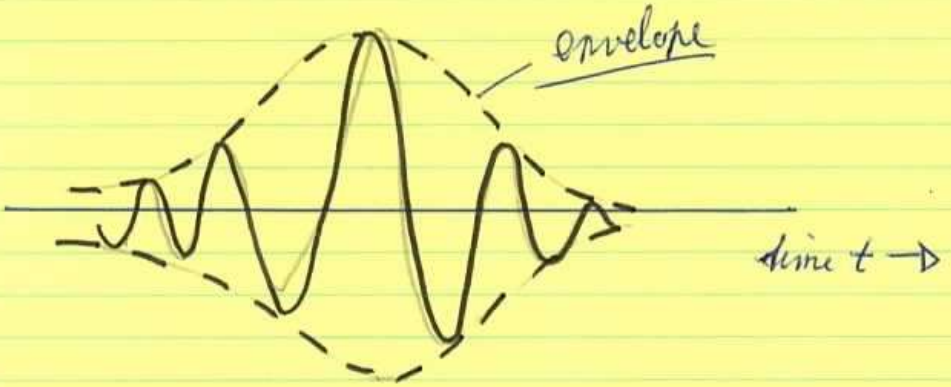

Benjamin-Feir Instability

Four-wave Interaction : $k_0 + \Delta k_0 + k_0 - \Delta k_0 = k_0 + k_0 = 2k_0$

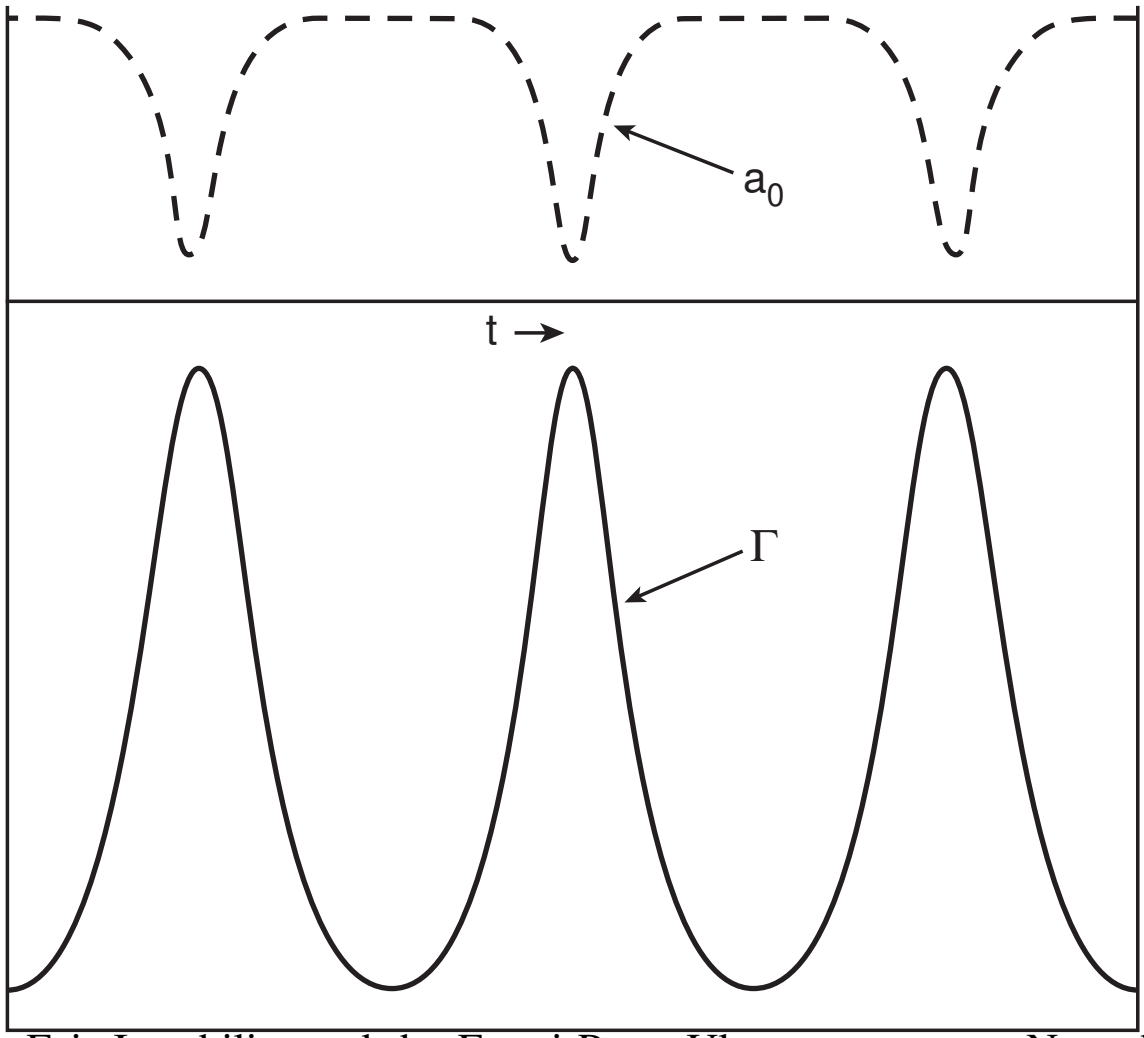

Figure 1: Benjamin-Feir Instability and the Fermi-Pasta Ulam recurrence. Note the interplay between carrier wave (a_0) and sideband (Γ).

Probability distribution function for envelope wave height

Theoretical development (see e.g. Gabor, Longuet-Higgins, Srokosz, Tayfun) is based on the statistics of the envelope ρ of a time series of the surface elevation η, where

$$\eta = \rho \cos\theta$$

For nonlinear waves the p.d.f. of η follows the Edgeworth expansion whose first term is the Gaussian distribution. Using this one finds for the normalized envelope wave height ($h = 2\rho/H_S$) p.d.f.

$$p(h) = 4he^{-2h^2}\left\{1 + C_4\left(2h^4 - 4h^2 + 1\right) + C_3^2\left(4h^6 - 18h^4 + 18h^2 - 3\right)\right\}.$$

where envelope skewness C_3 and kurtosis C_4 are known if the wave spectrum is known: $C_3 = \langle\eta^3\rangle/\eta^2\rangle^{3/2}$, while $C_4 = \langle\eta^4\rangle/3\langle\eta^2\rangle^2 - 1$.

Here, H_S is the significant wave height defined as $H_S = 4\sqrt{m_0}$ where $m_0 = \langle\eta^2\rangle$ is the variance of the sea surface elevation η.

The expressions for skewness and kurtosis can be obtained, in principle, from the **Hamiltonian** for water waves. This takes too much time to derive so I just give the end result. For example, the contribution to kurtosis by the **four-wave interactions** is found to be

$$C_4^{dyn} = \frac{4}{g^2 m_0^2} \int \mathrm{d}\mathbf{k}_{1,2,3,4} T_{1,2,3,4} \delta_{1+2-3-4} \left(\omega_1 \omega_2 \omega_3 \omega_4\right)^{\frac{1}{2}} \times R_r(\Delta\omega, t) N_1 N_2 N_3, \qquad (1)$$

where $R_r(\Delta\omega, t) = (1 - \cos(\Delta\omega t))/\Delta\omega$, $\Delta\omega = \omega_1 + \omega_2 - \omega_3 - \omega_4$, $\omega(k, D)$ is the dispersion relation for gravity waves which depends on wavenumber k and depth D, and $T_{1,2,3,4}$ is a complicated interaction coefficient while the action density $N(\mathbf{k}) = gF(\mathbf{k})/\omega$ with F the wavenumber spectrum.

Hence, deviations from **Gaussianity** are known in terms of the mean state. This expression gives the contribution of the free waves to the kurtosis, it is a six-dimensional integral and is therefore too expensive in an operational context.

Similar relations exist for the contributions of the bound waves to skewness and kurtosis.

Validation

Use Monte-Carlo simulations for surface gravity waves to validate the approach. The surface elevation η is given by

$$\eta = a\cos\theta + \alpha a^2 \cos 2\theta + \beta a^3 \cos 3\theta,$$

where α and β are known functions of wave number k_0 and depth D. Here, a 50,000,000 member ensemble is generated by drawing amplitude a from the Rayleigh distribution and phase θ from the uniform distribution (Random phase approximation).

The resulting pdf for envelope wave height has an exponential tail while nonlinear theory with added exponential tail shows good agreement with the numerical result.

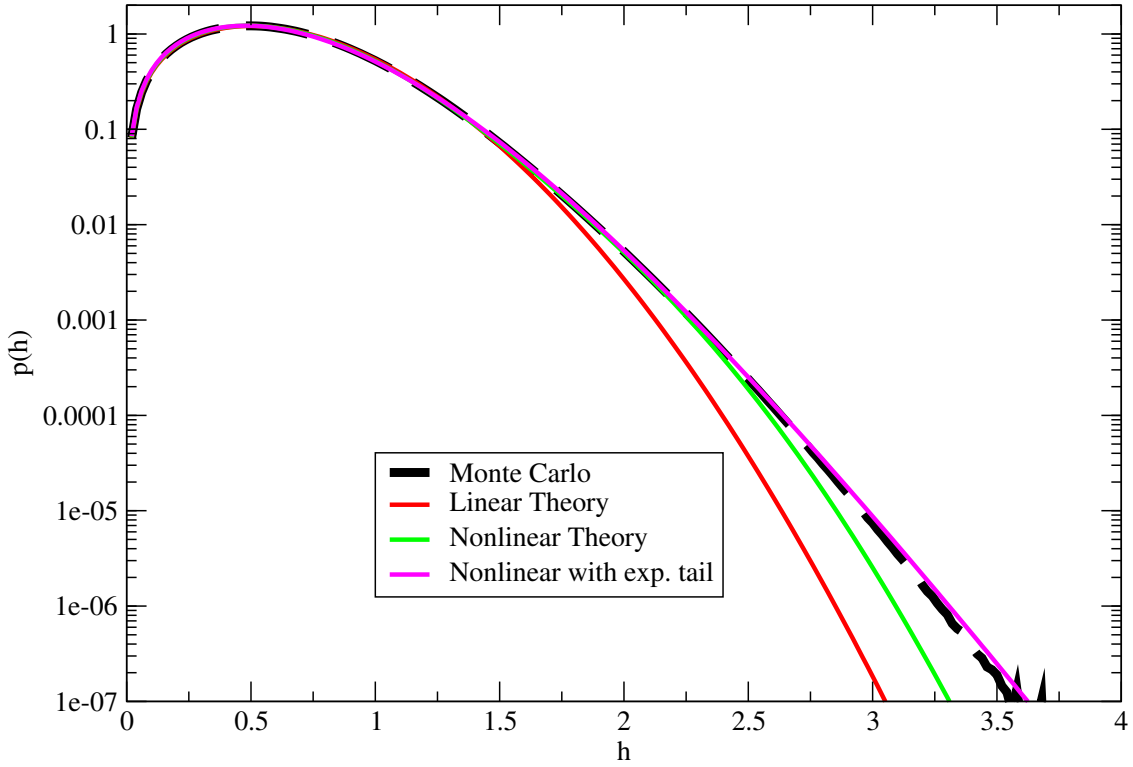

Figure 2: Probability distribution function of envelope wave height for a significant steepness of 0.06 and a dimensionless depth of 1.45, mimicking the Draupner wave event. The Monte Carlo simulation shows clear evidence that the tail of the distribution is exponential. Nonlinear theory combined with the stretched exponential of Residori is in good agreement with the simulation.

Parametrization of skewness and kurtosis.

A key step in the method is to obtain for given sea state statistical information such as envelope skewness and kurtosis. As already mentioned, their formula have been derived, but they are 4th and 6th dimensional integrals and therefore involve a large amount of computation. For operational applications a parametrization of these statistics is required.

I will treat the contributions by the bound-waves and the free waves separately, and I will validate the parametrizations against exact computations using simulated spectra of the **Draupner** freak wave event and the **Andrea** Storm. These spectra were generated with the coupled ECWAM-IFS system and were provided by Luciana, Gigi, Jean and Nils.

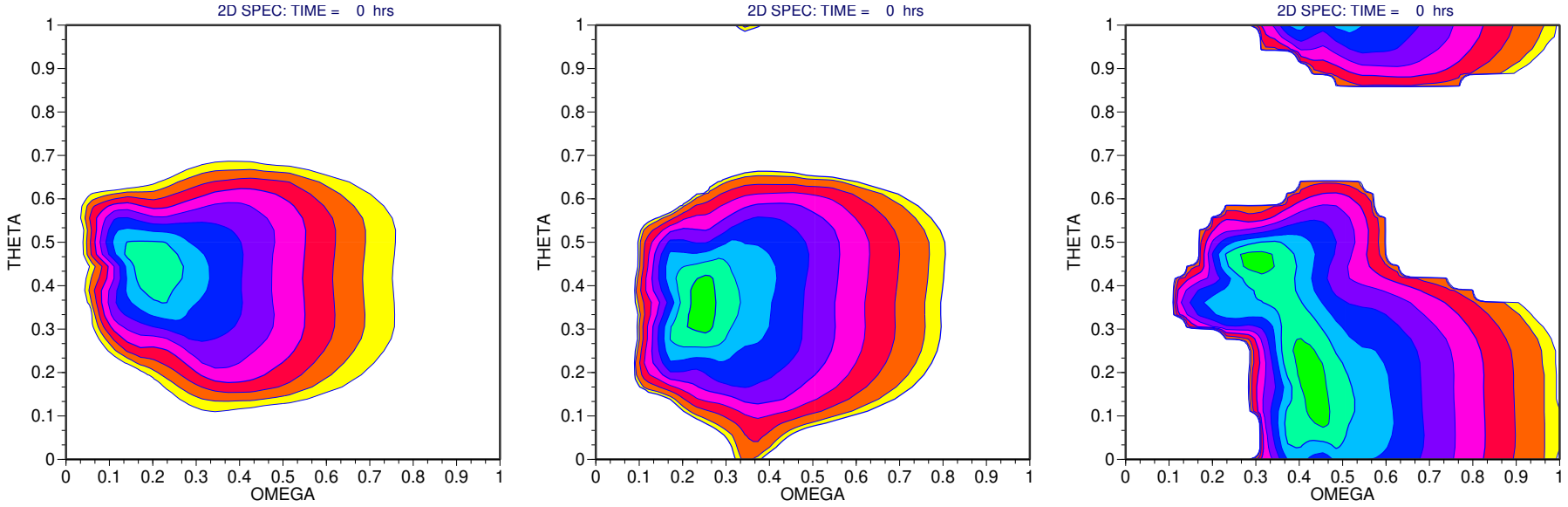

Figure 3: Left panel: Wave spectrum for Draupner event at 16:00 hrs on 1-1-1995; Middle panel: Andrea main event at midnight of 9-11-2007; Right panel: broad-band spectrum 12 hrs before the Andrea event.

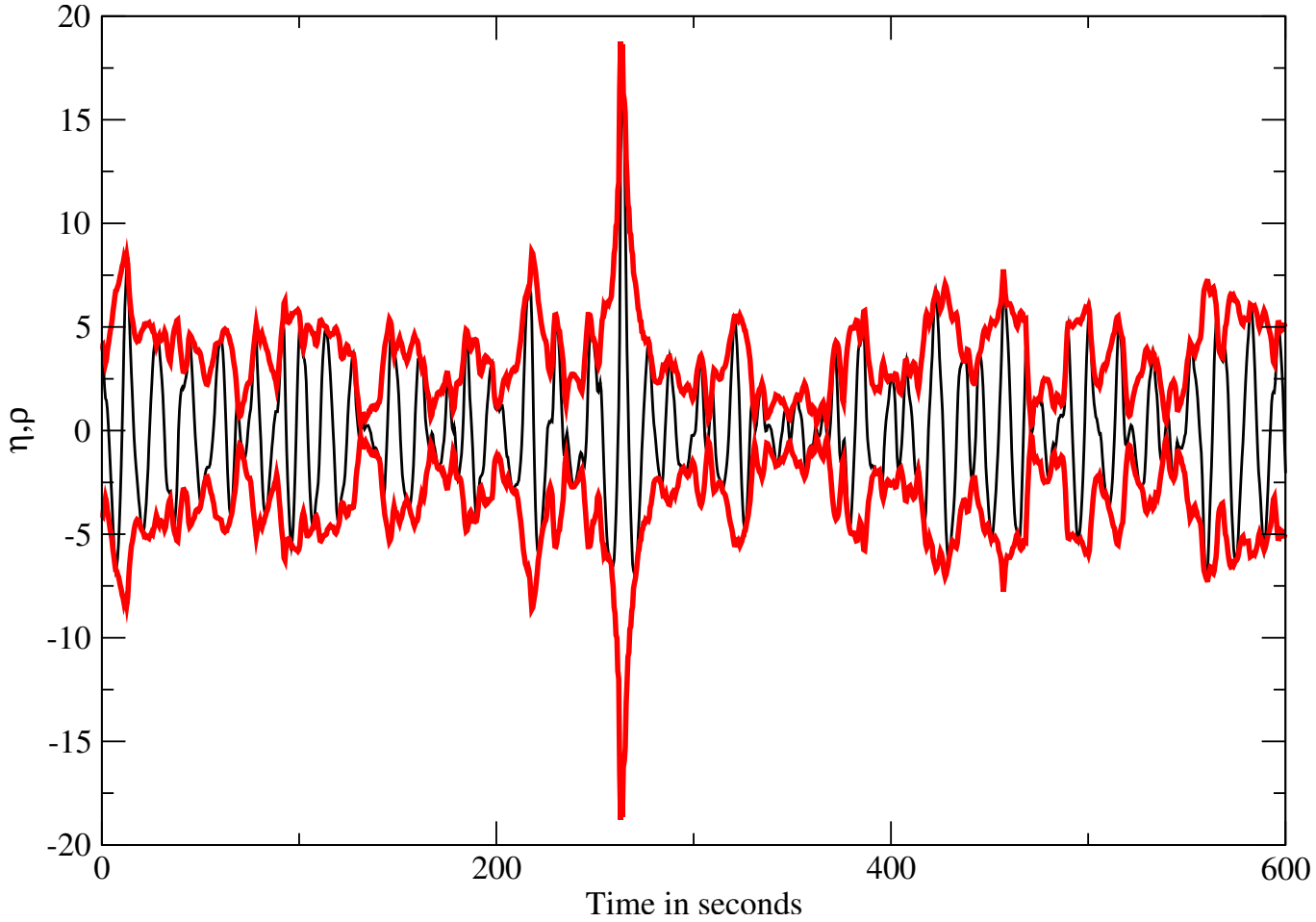

Figure 4: Draupner freak wave on January 1 1995. Shown are surface elevation η in black and envelope ρ in red

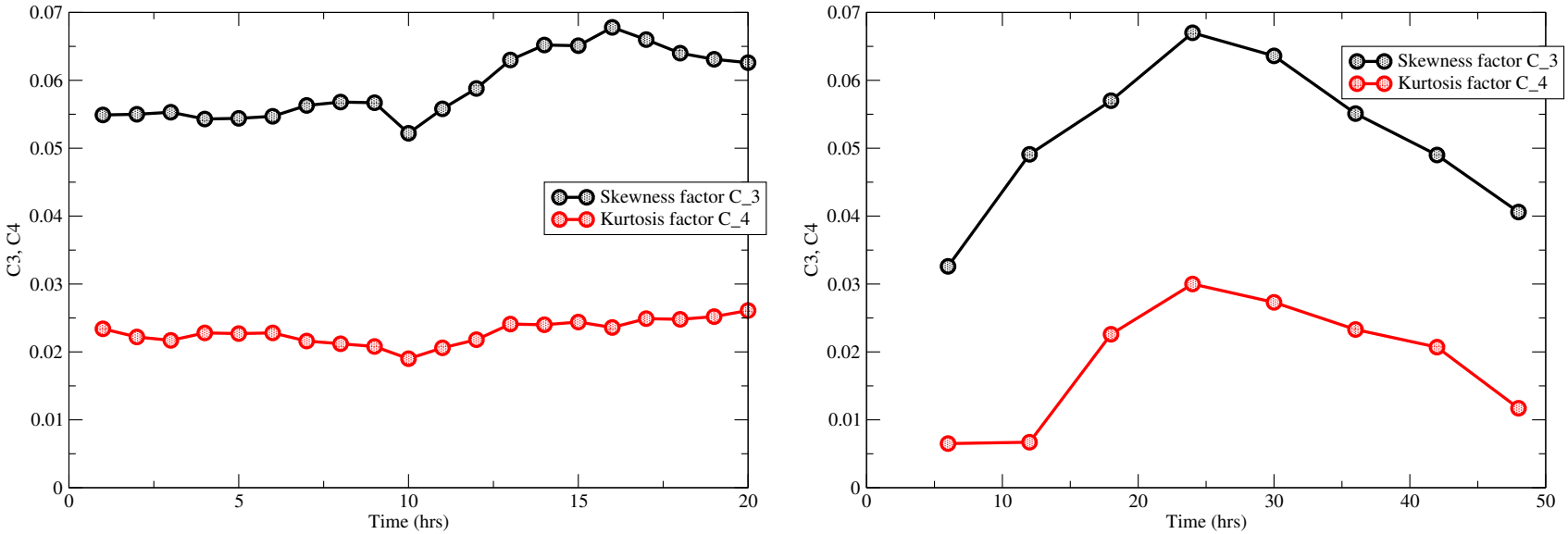

Figure 5: Evolution in time of skewness factor C_3 and kurtosis factor C_4 for the Draupner case (left panel) and the Andrea storm (right panel).

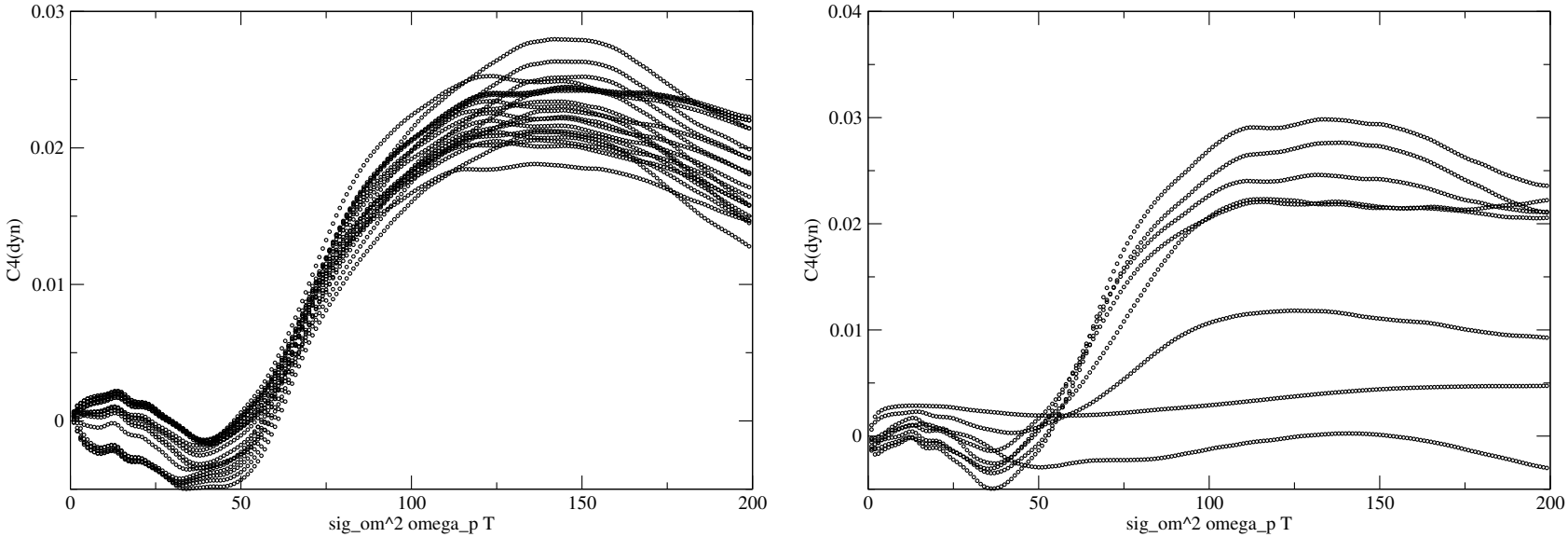

Figure 6: Evolution of dynamic kurtosis C_4^{dyn} as function of the dimensionless time $\tau = \sigma_\omega^2 \omega_p T$, where σ_ω is the relative width of the frequency spectrum and ω_p is the angular peak frequency. Left panel shows the Draupner case while the right panel shows the Andrea storm.

Exceedance probability

I will call the probability that maximum envelope wave height is larger than a critical value the **exceedance probability**. Assuming that the pdf of envelope wave height is known, and defining the cumulative distribution function as

$$P(h) = \int_h^\infty \mathrm{d}h \; p(h),$$

the exceedance probability becomes

$$P(h_{max} > h_c) \simeq 1 - \exp(\mathscr{G}(h_c)) = 1 - \exp(-NP(h_c)).$$

Here, the number of events N is essentially the number of wave groups. Following a method by Adler (1981) N is estimated for a domain of 14×14 km (the resolution of the wave model) and next the exceedance probability for **observed maximum wave height** is shown.

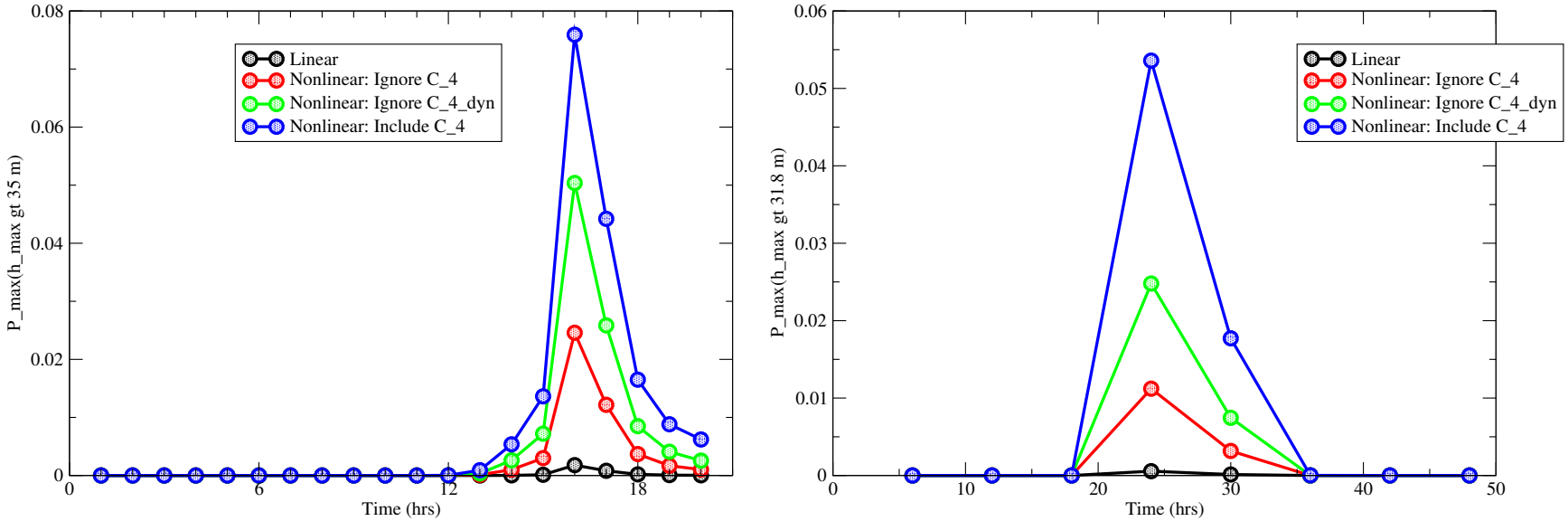

Figure 7: Evolution in time of simulated exceedance probability $P_{max}(h_{max}^{obs})$ for $h_{max}^{obs} = 35$ m (Draupner, left panel) and for $h_{max}^{obs} = 31.8$ (Andrea storm, right panel). For comparison the corresponding results from linear theory are shown, whereas also the impact of dynamic kurtosis and total kurtosis is depicted.

Bound-waves

In order to obtain parametrizations for the bound-wave contributions to skewness and kurtosis I start from the exact expressions for a **single** wave. It turns out that these functions depend on the steepness $\varepsilon = k_0 m_0^{1/2}$ and the dimensionless depth $x = k_0 D$. In order to apply the single-wave formula to the case of general spectra I have modified the definition of the steepness and dimensionless depth by using instead of the peak wavenumber k_0 the mean wavenumber k_{mean} obtained by using the mean angular frequency in the inverse of the dispersion relation. After adjusting the coefficients I obtained

$$C_3^{bound} = 2.24\varepsilon\left(\alpha + 0.9\Delta\right),\; C_4^{bound} = 7.42\varepsilon^2\left\{\gamma + \alpha^2 + \left(\alpha+\Delta\right)^2\right\},$$

where $\alpha(x)$, $\gamma(x)$ and $\Delta(x)$ are known functions of dimensionless depth x.

Validate against exact expression using simulated spectra from Draupner and Andrea.

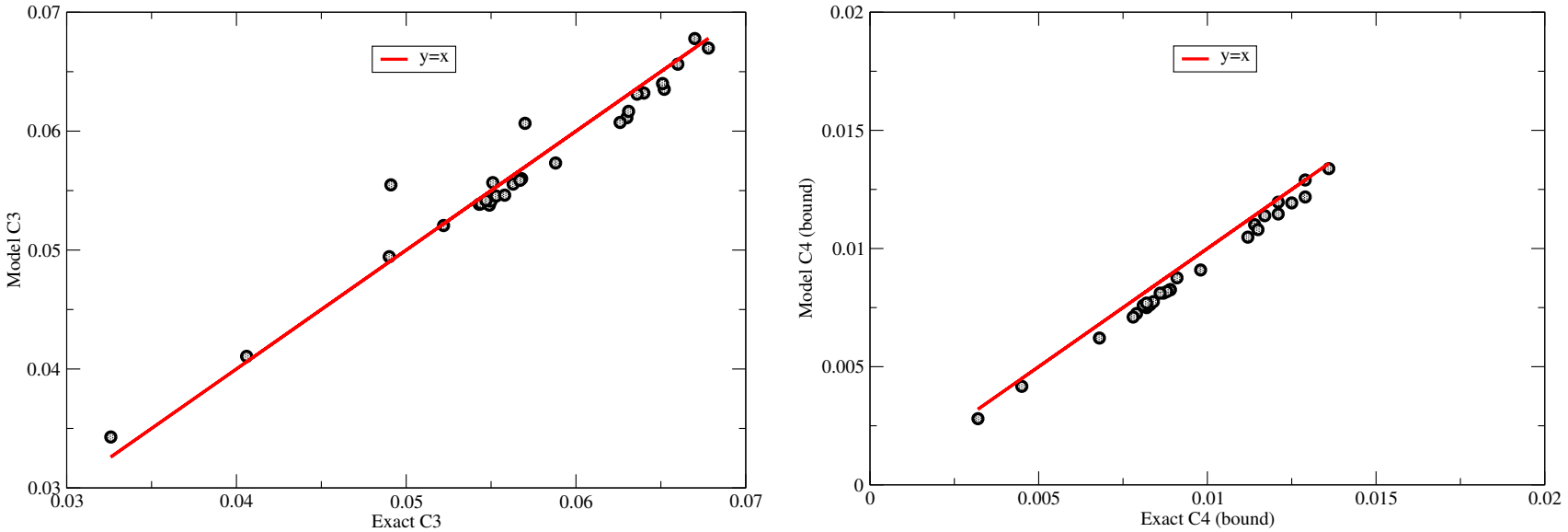

Figure 8: The left panel shows the comparison of parametrized skewness factor C_3^{bound} against exact computation from the Draupner and Andrea events, while the right panel shows the comparison for the kurtosis factor C_4^{bound}.

Free-waves

Free-waves only give rise to kurtosis, because they are subject to four-wave interactions, which is a third order nonlinearity.

As a guide for parametrization I have used exact results for the case of a narrow-band spectrum of Gaussian shape with frequency width δ_ω and directional width δ_θ. This problem is determined by two parameters. Including shallow water effects the first one is the Benjamin-Feir Index BFI, defined as

$$BFI^2 = \frac{2\varepsilon^2}{\delta_\omega^2} \times F(x) \tag{2}$$

where $F(x)$ is a known function of dimensionless depth $x = k_0 D$, which is proportional to the nonlinear interaction coefficient. In 1D $F(x)$ vanishes for $x = 1.363$, but for 2D this is not true. In fact, there is noticable Benjamin-Feir Instability down to $x = 0.5$. The second parameter measures the importance of directional versus frequency width. It reads

$$R = 0.5 \frac{\delta_\theta^2}{\delta_\omega^2} \times G(x) \tag{3}$$

where $G(x)$ depends on dimensional depth and is for $x \simeq 1.5 - 2$ of the order 0.75.

In the narrow-band approximation the parameter C_4^{free} becomes

$$C_4^{free} = J(R,\tau)BFI^2, \tag{4}$$

where

$$J(R,\tau) = 2\int \mathrm{d}\nu_{1,2,3}\mathrm{d}\phi_{1,2,3}E_1E_2E_3G(\Delta\omega,\tau), \tag{5}$$

with resonance function $G(\Delta\omega,\tau) = (1-\cos(\Delta\omega\tau)/\Delta\omega$. Here, $\tau = \delta_\omega^2\omega_0 t$ is dimensionless time, and $\Delta\omega = (\nu_3-\nu_1)(\nu_3-\nu_2) - R(\phi_3-\phi_1)(\phi_3-\phi_2)$. The frequency parameter ν and direction parameter ϕ have been made dimensionless by means of the frequency width and the directional width.

For a Gaussian spectrum the integrals in (5) may be evaluated exactly (Fedele, 2015) and the result is shown next.

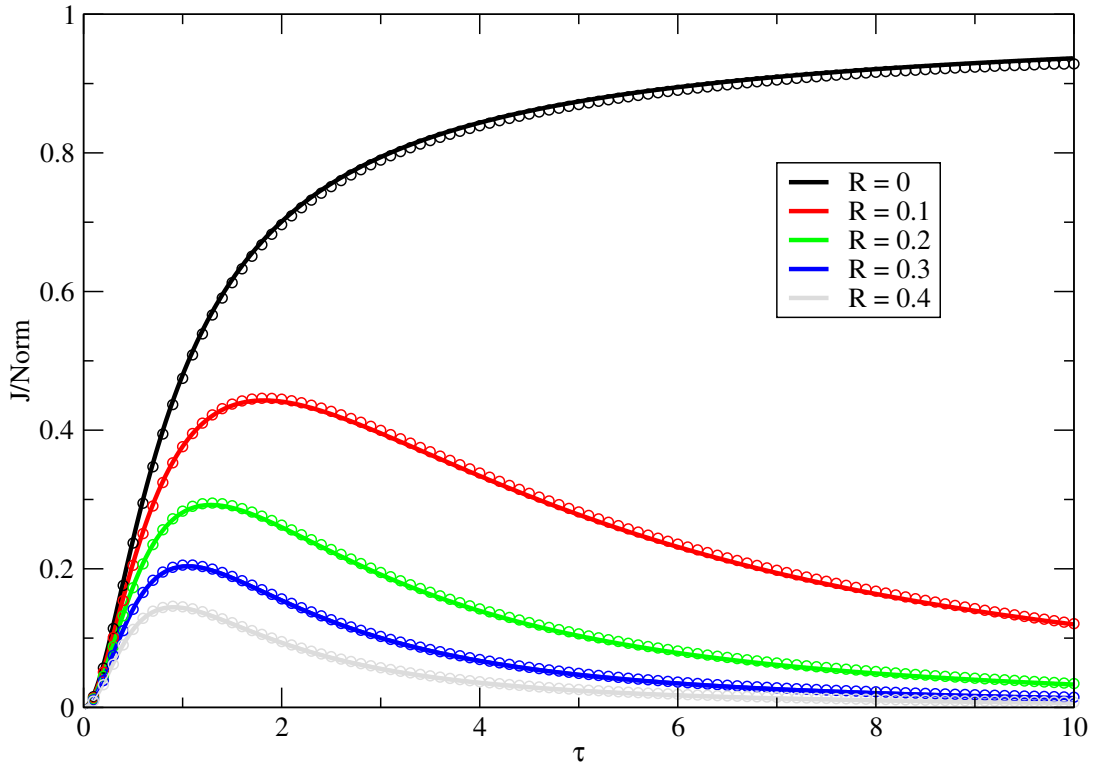

Figure 9: Evolution of normalized kurtosis $C_4/(Norm \times BFI^2)$, with $Norm = \pi/3\sqrt{3}$, versus dimensionless time for different values of R. Results using the numerical solution of (5) are shown as the full lines.

From the plot it is clear, that for Gaussian spectra the kurtosis parameter C_4^{free} has a maximum after which it decays to zero for large times. As an indicator of the severity of the weakly nonlinear sea state one could use the maximum value of J. In next Figure I have plotted the maximum as function of R. Also shown is the fit

$$\frac{J}{N} = \frac{R_0(1-R)}{R+R_0}, \; N = \frac{\pi}{3\sqrt{3}}, \tag{6}$$

with $R_0 = 7.44\sqrt{3}/4\pi^3$, and the fit approximates the 'exact' results reasonably well. A better fit was found by Janssen & Janssen (2018)

$$\frac{J(R)}{N} \quad = \quad \left(1 - \alpha\sqrt{R} + \beta R + \delta R^2\right), \; 0 < R < 1, \tag{7}$$

where $\alpha = 4\sqrt{3}/\pi$ and $\beta = (1/3 + 2\sqrt{3}/\pi)$, and δ is chosen such that $J(R)$ at $R = 1$ satisfies the exact result that $J(R)$ vanishes.

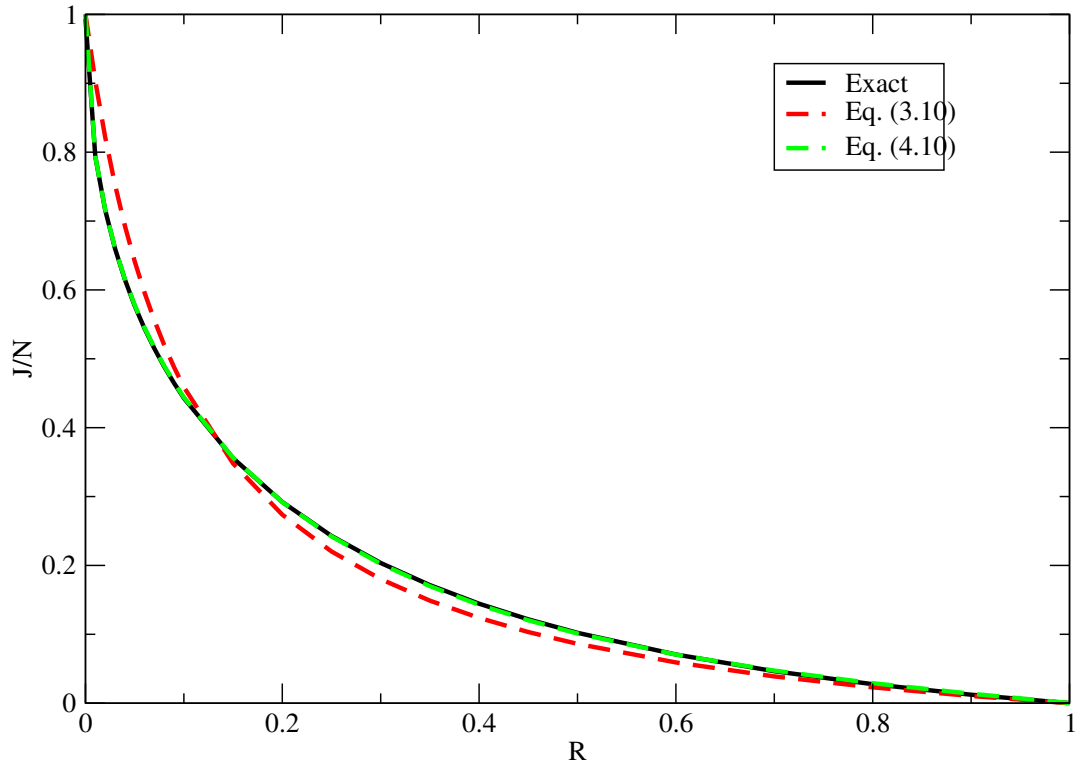

Figure 10: Maximum value of J versus R. The fits (6) and (7) are shown as well.

As a basis for parametrization the average of the free-wave kurtosis I will use

$$C_4^{free} = J(R) \times BFI^2, \tag{8}$$

where

$$\frac{J(R)}{N} = 0.9\left(1 - \alpha\sqrt{R} + \beta R + \delta R^2\right),\ 0 < R < 1, \tag{9}$$

and to accommodate 'general' spectra I replace the parameters R and BFI by appropriate spectral averages. This parametrization shows a reasonable agreement with the exact computations shown next.

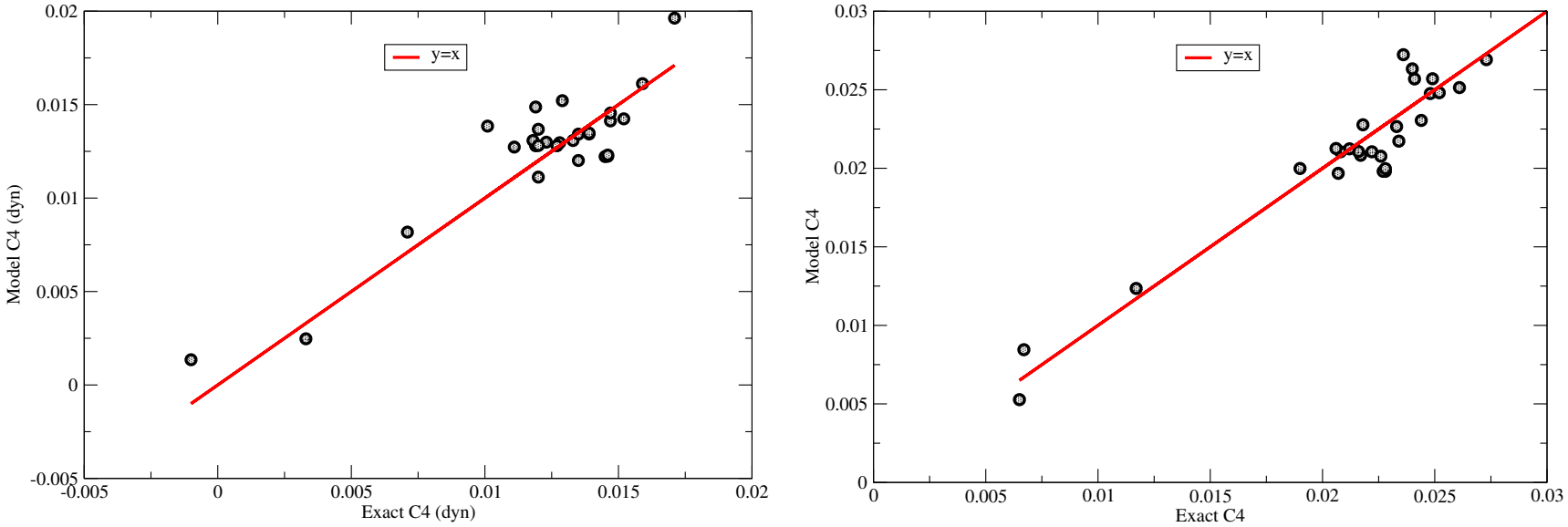

Figure 11: The left panel shows the comparison of parametrized dynamic kurtosis factor C_4^{dyn} against exact computations using spectra from the Draupner and Andrea events, while the right panel shows the comparison for the total kurtosis factor C_4.

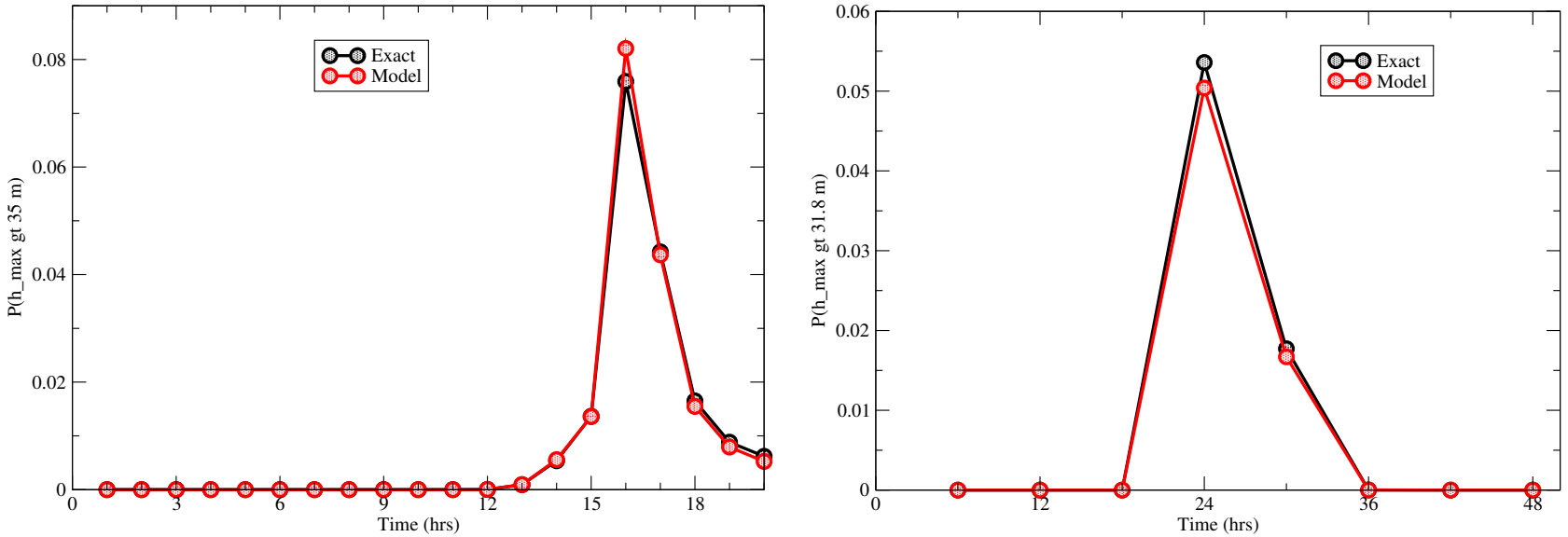

Figure 12: Comparison of parametrized exceedance probability $P_{max}(h^{obs}_{max})$ for $h^{obs}_{max} = 35$ m (Draupner, left panel) and for $h^{obs}_{max} = 31.8$ (Andrea storm, right panel) with numerical computations using the exact theory.

Shallow water effects.

I have noted that in shallow water ($kD = O(1.5-2)$) the wave spectra have a fairly narrow directional distribution. This has consequences for freak wave generation. This is illustrated by a single-gridpoint run where we compare for deep and shallow ($D = 40m$) water the evolution of dynamic kurtosis.

Note that for narrow directional spectra with $R < 1$ dynamic kurtosis will be positive, this may occur in shallow water, as seen in the next Figure. In deep water, with broader directional spectra R is around 1 and kurtosis is seen to be small.

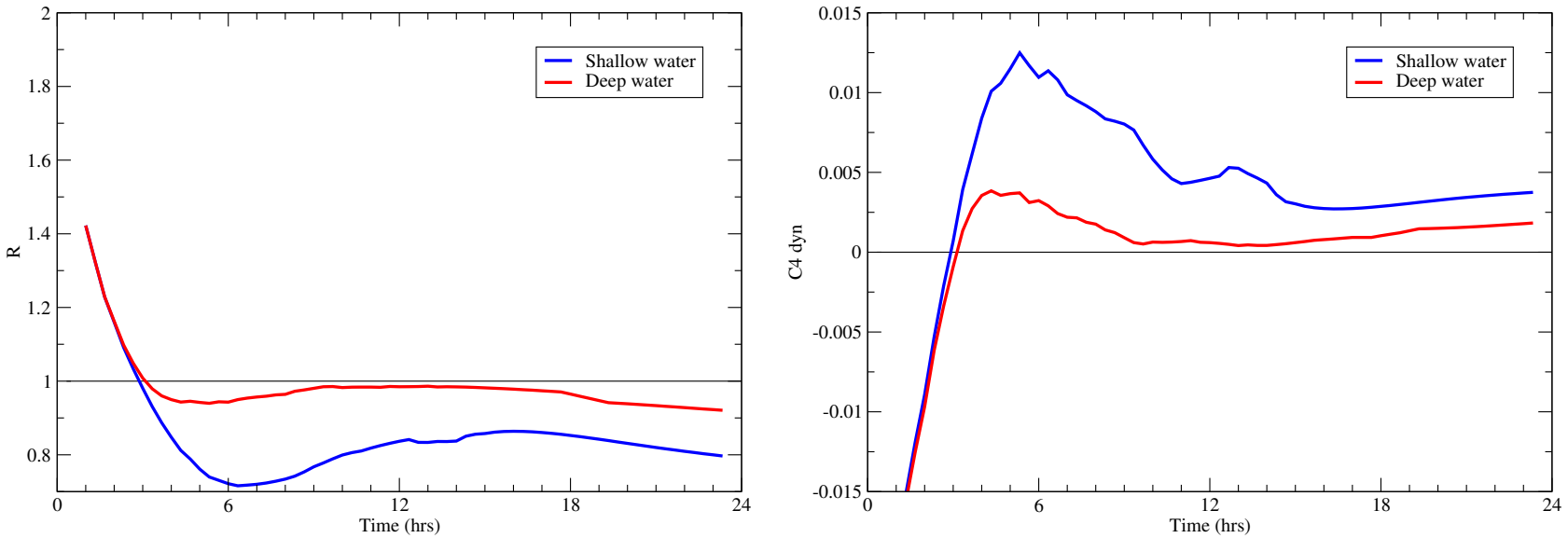

Figure 13: Left Panel: Comparison of time-evolution of normalized width parameter R for deep and shallow water. The threshold value of $\alpha = 1$ is indicated as well. Right panel: Comparison of time-evolution of dynamic kurtosis for deep and shallow water.

A Synoptic example.

Jean Bidlot and I have implemented these changes in our operational software and here I show results such as the relation of statistics with wave age and the global average of maximum wave height pdf.

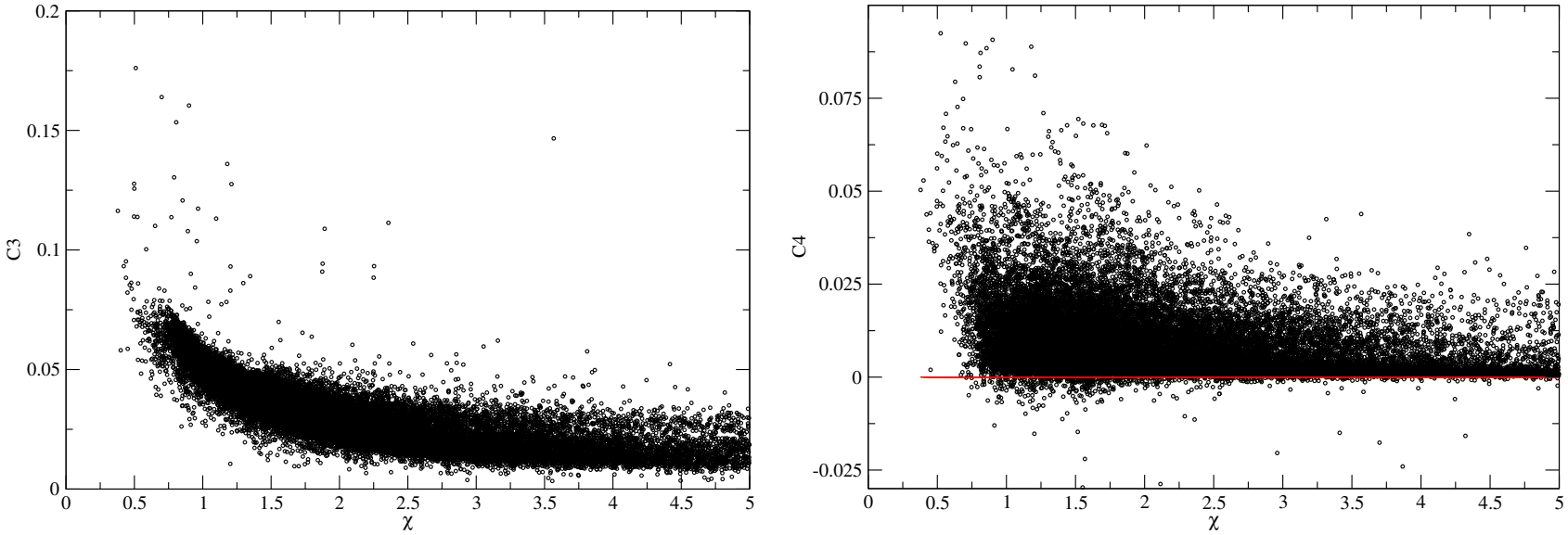

Figure 14: Skewness factor C_3 (left panel) and kurtosis factor C_4 (right panel) versus wave age parameter $\chi = c_p/U_{10}$. Note that there are a number of occasions where the directional wave spectrum is so broad that kurtosis is slightly negative.

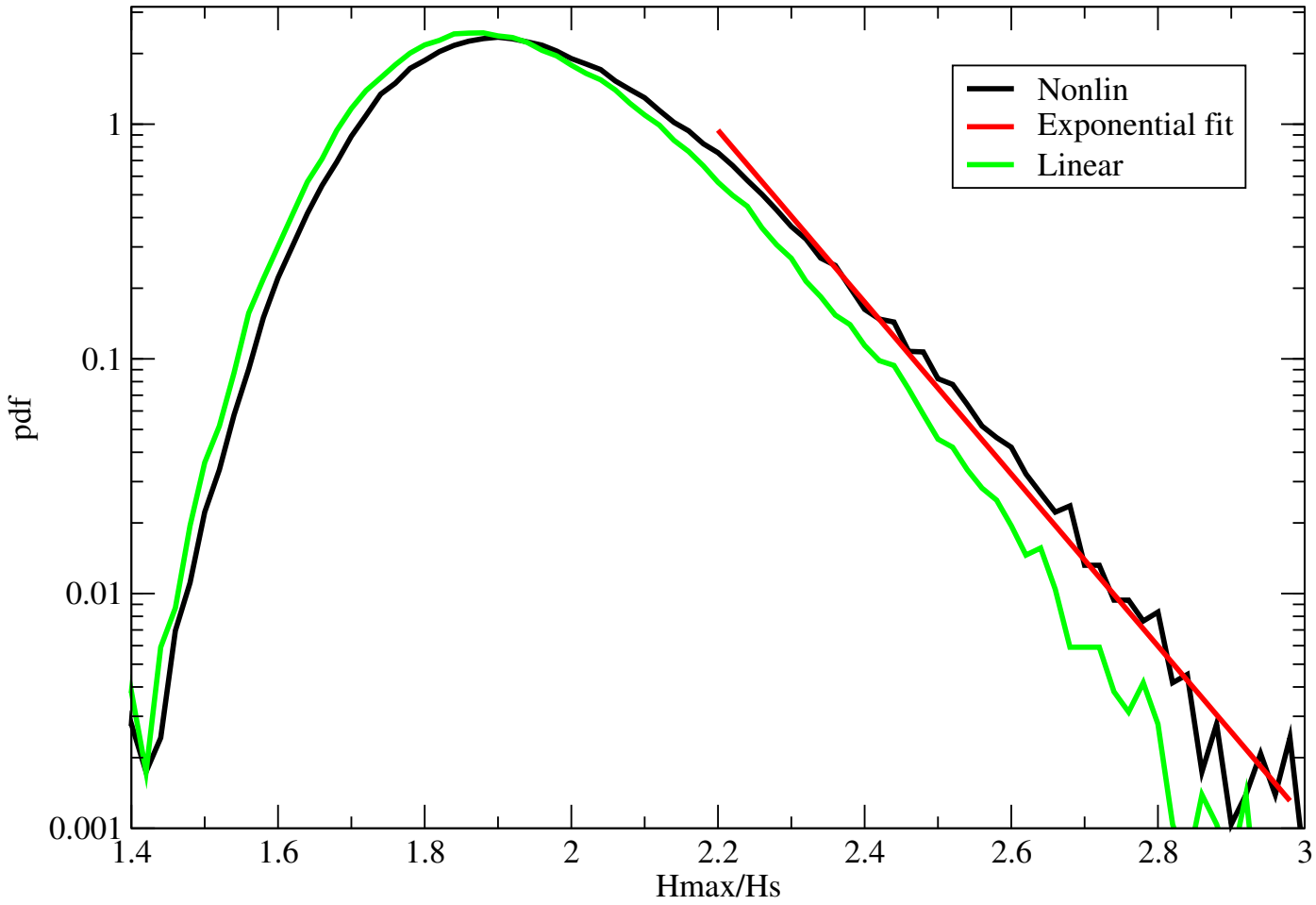

Figure 15: Global maximum wave height distribution obtained by a random draw of H_{max} for given number of waves and given skewness and kurtosis. Including skewness and kurtosis shows that the tail of the distribution is exponential. The distribution according linear theory is shown as well.

Conclusions.

- An efficient parametrization of skewness and kurtosis of surface gravity waves, including shallow water effects, has been obtained.
- For the Draupner and Andrea cases effects of skewness and kurtosis are equally important in determining exceedance probabilities for maximum envelope wave height.
- For intermediate water depth dynamic kurtosis is still relevant. One reason is that in 2D there is still Benjamin-Feir instability for dimensionless depth $k_0 D < 1.363$. The other reason is that in this depth range wave spectra have a surprisingly narrow directional distribution.